Engineering Physics
2018; 2(1): 6-10
http://www.sciencepublishinggroup.com/j/ep
doi: 10.11648/j.ep.20180201.12

Microstructural Characterization of $Ti_{20}Zr_{20}Cu_{40}Ni_{20}$ Metallic Glass

Panugothu Rama Rao[1, 2, *], Anil Kumar Bhatnagar[3], Bhaskar Majumdar[4]

[1]School of Engineering Sciences & Technology, University of Hyderabad, Hyderabad, India

[2]CSIR-Central Glass and Ceramic Research Institute, Kolkata, India

[3]School of Physics, University of Hyderabad, Hyderabad, India

[4]Defence Metallurgical Research Laboratory, Kanchanbagh, Hyderabad, India

Email address:
panugothu.ramarao@gmail.com (P. R. Rao)

[*]Corresponding author

To cite this article:
Panugothu Rama Rao, Anil Kumar Bhatnagar, Bhaskar Majumdar. Microstructural Characterization of $Ti_{20}Zr_{20}Cu_{40}Ni_{20}$ Metallic Glass. *Engineering Physics*. Vol. 2, No. 1, 2018, pp. 6-10. doi: 10.11648/j.ep.20180201.12

Received: March 13, 2018; **Accepted**: March 28, 2018; **Published**: May 4, 2018

Abstract: In the present investigation, we present our results on characterization of Ti joints, brazed with metallic glass ribbons of $Ti_{20}Zr_{20}Cu_{40}Ni_{20}$ alloy. Initially, metallic glass ribbons were produced using a vacuum melt spinner and used as filler materials for vacuum brazing of two Ti alloy plates at 1270 K. Field-Emission Scanning Electron Microscopy (FESEM), the as-spun ribbons showed fully amorphous structure when examined on both surfaces by XRD and also verified by TEM investigation. The detailed DSC results revealed that the amorphous phase crystallized at approximately 753K. The brazing joint of two Ti-plates using the metallic glass ribbon was found to be very sound. FESEM characterization of the cross-sectioned brazing joint shows sub-micron size grains uniformly distributed in the matrix with brighter appearance. EDX analysis revealed that the sub-micron grains are rich in Ti, while the matrix phase has Zr-enrichment. Back Scattered Electron (BSE) image also suggested substantial reaction of the brazing ribbon with Ti plates, whose typical lath microstructure is modified to nanostructured lamellar eutectic microstructure comprising of Ti-rich and Zr-enriched phases.

Keywords: Metallic Glass, Brazing, Scanning Electron Microscopy, Energy Dispersive Spectroscopy

1. Introduction

Titanium alloys, due to their high specific strength and good corrosion resistance, are particularly suitable for special applications [1-4]. CP-Ti (Commercially Pure Titanium), which is unalloyed, ranges in purity from 99.5 to 99.0 (wt%) Ti, titanium exists in two allotropic crystal structures. There are hexagonal close-packed (HCP) structure-α, and body-centered cubic (BCC) crystal structure-β. Above the β-transition temperature, the hexagonal α-phase is transformed on heating to the BCC β-phase [3-4]. It has been reported that the Ti alloys are successfully brazed using the Ti-based braze alloys, Ti-Cu-Ni and Ti-Zr-Cu-Ni alloy systems [5-7]. Investigations on the formation and properties of amorphous alloys by rapid quenching have formed an important branch of recent metallurgical research activities. Metallic glasses continue to attract attention of R&D workers due to their possible applications in diverse areas. Ferromagnetic glasses have been studied extensively for many years due to their possible applications as well as from scientific points of view. One of the important properties of metallic glasses is their thermal stability because on heating beyond a certain high temperature and/or for an extended time at moderate temperatures, metallic glasses show degradation of most of their properties. In this work, we report studies on microstructural and thermal stability of $Ti_{20}Zr_{20}Cu_{40}Ni_{20}$.

2. Experimental Methods

The alloy with nominal composition $Ti_{20}Zr_{20}Cu_{40}Ni_{20}$ is prepared from pure elements (purity > 99.9 wt.%) by arc melting in a titanium-gettered argon atmosphere. For achieving homogeneity in the alloy composition, it is re-melted many times. The amorphous ribbon of this compound

is prepared using the standard rapid quenching technique. The ribbon is about 25 mm wide and 100 μm thick. The X-ray Diffractometers, used to characterize the sample, is a Bruker machine, Model No**.** D8. The thermal stability of the melt spun ribbon is carried out using a (DSC 821, METTLER – Toledo) Differential Scanning Calorimeter (DSC). Scans were performed using a constant heating rate of 10 K/min. The Field Emission Gun (FEG) is usually a wire of Tungsten (W) Zigma, Carl Zeiss, Germany (FE-SEM, Carl ZEISS, FEG, Ultra 55), 30kV, images were obtained at an operating voltage of 15 kV and the working distance was about 8.5 mm.

Vacuum brazing was performed to braze commercially pure CP-Ti plates using the as spun $Ti_{20}Zr_{20}Cu_{40}Ni_{20}$ metallic glass ribbon as filler material. The CP-Ti plates measuring 10 mm×7 mm× 3mm were prepared. the lap-butt joint, the CP-Ti plates measuring 5 mm×3 mm×1 mm were first prepared and then steps were cut in EDM using a 0.5 mm wire. Both the brazing ribbons and Ti plates were initially cleaned using acetone and then the ribbons were kept in between the two Ti plates before tightening them using nicrome wire. The samples were then placed in a vacuum furnace (10^{-3} mbar) and annealed for 10 minutes. The selected temperature for each sample was 20±5°C higher than the solidus temperature of respective ribbon. The samples were then furnace cooled.

3. Results and Discussion

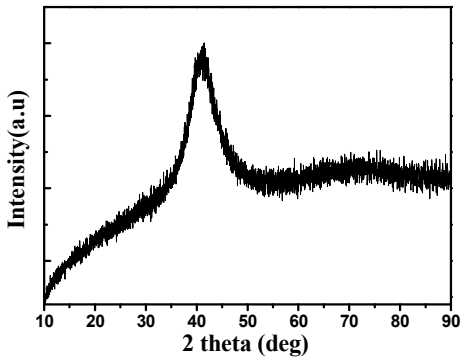

Figure 1. *XRD patterns of as-cast metallic glass $Ti_{20}Zr_{20}Cu_{40}Ni_{20}$ sample.*

Figure 1 shows the XRD pattern of the as-spun ribbon of $Ti_{20}Zr_{20}Cu_{40}Ni_{20}$. It shows a typical broad maximum, characteristic of amorphous/glassy materials and no distinct crystalline peaks are observed within the sensitivity limits of the diffractometer. This confirms the glass formation of $Ti_{20}Zr_{20}Cu_{40}Ni_{20}$in the ribbon form. Figure 2 shows the DSC curve for this metallic glass at heating rates, i.e.10 K/min under non-isothermal conditions. It is observed that the crystallization of $Ti_{20}Zr_{20}Cu_{40}Ni_{20}$ metallic glass occurs in single step. The crystallization onset temperature T_x, and exothermic peak temperatures T_p, at which peaks appear in the DSC thermograms.

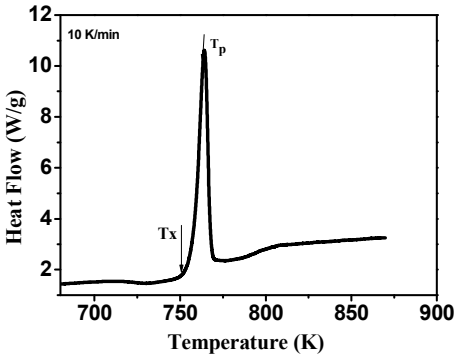

Figure 2. *DSC curve of the $Ti_{20}Zr_{20}Cu_{40}Ni_{20}$ Metallic glass at 10 K/Min heating rate.*

The FESEM images of the interface microstructures of Ti/ $Ti_{20}Zr_{20}Cu_{40}Ni_{20}$ /Ti composite joint brazed at

1270 K for 10 min elucidating the Ti rich diffusion zones 1, 2, 3 and 4 (Figure 3 (a)-(d)) the reaction zone and the central zones are also shown respectively. To have an approximate idea of the elemental compositions of these regions, EDX spectrum 1 was taken from Ti-rich phase shown in Figure 3 (a), EDX spectrum 2 was taken from the $NiTi_2$ rich phase shown in Figure3 (b), EDX spectrum 3 was taken from the α-Ti shown in Figure 3 (c) and EDX spectrum 4 was taken from Ti_2Cu rich region shown in Figure 3 (d). The approximate average chemical compositions obtained from EDX experiments are shown in Table 1.

Thus, based on the experimental data displayed in Figures 3 and Table 1, it appears plausible to suggest the following processes to have occurred during the brazed joint formation. Dissolution of CP-Ti substrate into the brazed melt had possibly resulted in isothermal solidification of the molten brazed and had eventually formed primary β-Ti during brazing. The residual melt was solidified via eutectic reaction upon the cooling cycle of brazing. Based on the data of Table 1, the eutectic consisted most probably of $(Ti, Zr)_2Ni$, $NiTi_2$, Ti_2Cu, α-Ti, Eutectoid and Ti-rich as displayed in Figure 3 (a-g).

Table 1. *EDX analyses Based Elemental Chemical Composition Analysis of interface microstructures of Ti/ $Ti_{20}Zr_{20}Cu_{40}Ni_{20}$/Ti composite joint brazed at 1270 K for 10 min.*

Area	Elements (at.%)				
	Ti	Zr	Cu	Ni	Phases
I	91.98	04.80	01.92	01.38	Ti-rich
II	65.11	03.81	29.90	05.53	α-Ti
1	49.69	20.24	15.71	14.36	Eutectoid
2	49.44	20.49	15.80	14.28	$(Ti, Zr)_2Ni$ [8]
3	54.92	9.88	27.33	07.88	Ti_2CuRef [9]
4	55.85	9.05	27.06	08.04	$NiTi_2Ref$ [10]

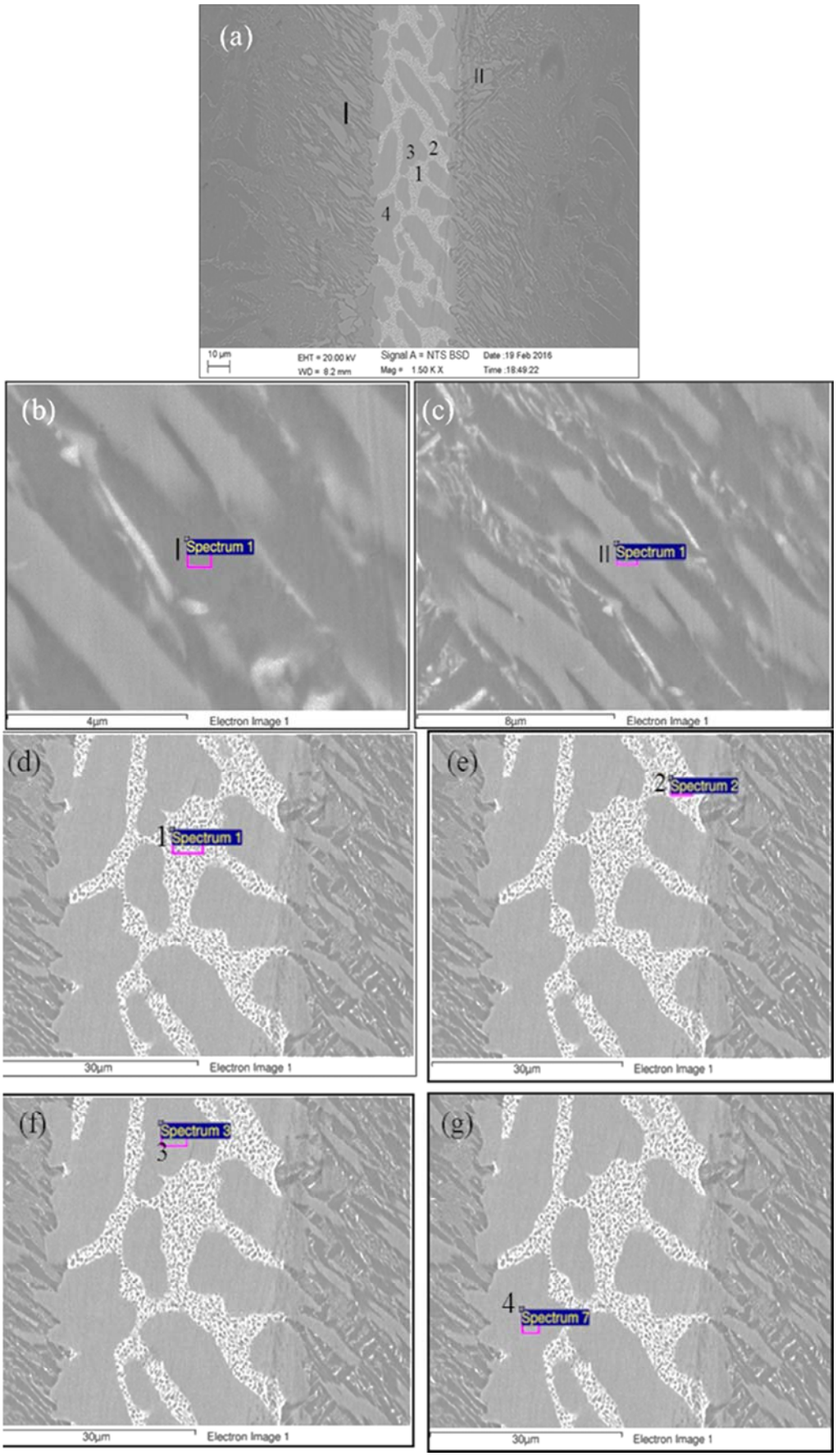

Figure 3. *Further FESEM study of the interface microstructures of Ti/$Ti_{20}Zr_{20}Cu_{40}Ni_{20}$/Ti composite joint brazed at 1270 K for 10 min:(a) cross-sectional overview of the joint (b)-(e): higher magnification of area I and II, (d) Diffusion zone 1, (e) diffusion zone 2, (f) Diffusion zone 3 and (g) Diffusion zone 4.*

Maximum solubilities of Cu and Ni in the β-Ti are 26.5 and 17 (at. %,) respectively. In contrast, Cu and Ni are dissolved in α-Ti up to 2.4 and (0.4 at.%) respectively. These values are significantly lower than their respective solubilities in β-Ti. Both Cu and Ni are hence well known to be stabilizers of the β phase in CP-Titanium. On cooling to room temperature, formation of both β-phase and intermetallic compounds may take place. Accordingly, decomposition of the β-Ti phase might have proceeded most likely via eutectoid solid-state transformation upon the cooling cycle of brazing. The eutectoid of $NiTi_2$, Ti_2Cu, α-Ti and Ti-rich might therefore have formed at room temperature in the earlier β-Ti grains of the brazed joint.

Higher brazing temperature resulted possibly in higher volume fraction of the β-Ti in the joint. This process had greatly enhanced the depletion rates of Cu, Ni, and Zr from the brazed melt into CP-Ti substrate during brazing. Because Cu, Ni, and Zr are all dissolved in the β-Ti, isothermal solidification of brazed melt during brazing resulted in formation of only β-Ti in the joint. Thus, the eutectic of $NiTi_2$, Ti_2Cu, α-Ti and Ti-rich phases had most likely disappeared from the brazed zone. The β-Ti alloyed with Cu, Ni, and Zr was therefore most likely to have had transformed to fine eutectoid of $NiTi_2$, Ti_2Cu, α-Ti and Ti-rich phases upon the subsequent cooling cycle of brazing. It is expected that the disappearance of coarse eutectic intermetallic compounds from the brazed zone is beneficial for enhancing the bond strength of the joint.

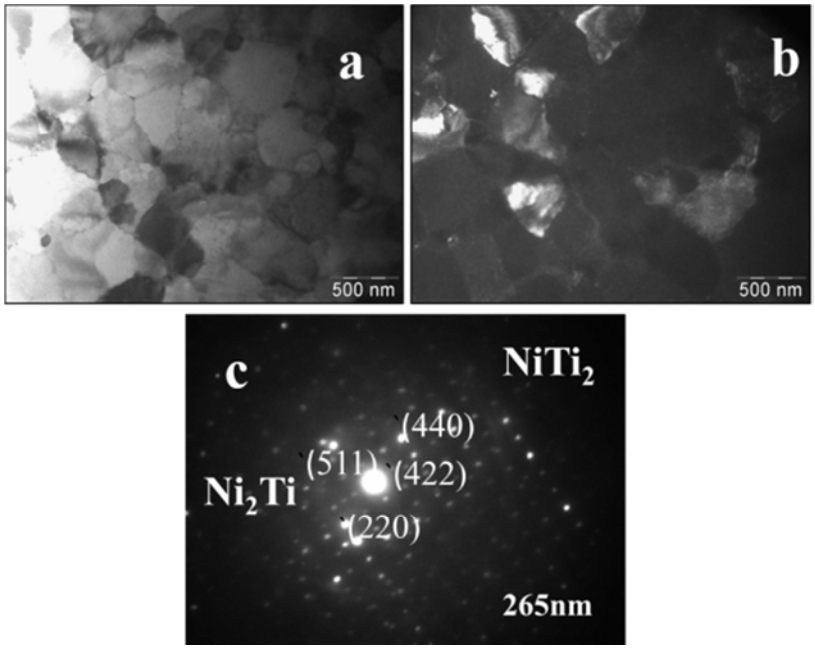

Figure 4. *TEM images of the $Ti_{20}Zr_{20}Cu_{40}Ni_{20}$ Metallic glass Ribbons annealed at 753K for 30 min (a) BF image, (b) DF image and (C) selected area electron diffraction patterns (SAED).*

Table 2. *Compositional Analysis of the $Ti_{20}Zr_{20}Cu_{40}Ni_{20}$ Metallic glass Ribbons annealed at 753 K for 30 min.*

Elements (at.%)				
Ti	Zr	Cu	Ni	Phase
18.14	22.13	38.45	21.26	Ni_2Ti & $NiTi_2$

The bright filed, dark filed and corresponding selected area electron diffraction patterns (SAED) of the $Ti_{20}Zr_{20}Cu_{40}Ni_{20}$ Metallic glass Ribbons annealed at 753 K for 30min are shown in Figures 4 (a), (b) and (c), respectively (8, 9). Table2 presents the corresponding data on compositional analysis of the same Ribbons annealed at 753K for 30 min. These results e.g., Figure. 4 (c) and Table 2 corroborated with the corresponding XRD data (Figure. 5). Figure 4 (a) and (b) confirmed the homogeneous distribution of the various nanocrystalline phases in the amorphous matrix. The existence of these nanocrystallie phases were confirmed from both the XRD data (Figure. 5) and the compositional analysis data obtained from the TEM studies (Table 2). The range of the size of spherical features in the dark field image (Figure 4b) was about 10 to 100nm

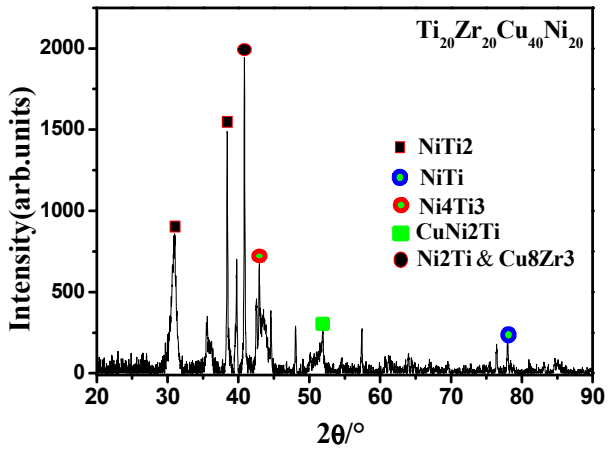

Figure 5. *XRD spectra of the $Ti_{20}Zr_{20}Cu_{40}Ni_{20}$ Metallic glass Ribbons annealed at 753 K for 30min.*

The XRD spectra shown in Figure 5 confirmed that annealing at 753K for 30 min produced the crystalline phases $NiTi_2$, NiTi, Ni_4Ti_3, $CuNi_2Ti$, Ni_2Ti and Cu_8Zr_3in the $Ti_{20}Zr_{20}Cu_{40}Ni_{20}$ metallic glass ribbons (10). The annealing temperature corresponded to the onset of crystallization temperature (T_x) of the exothermic peak on DSC curve (Figure. 2).

4. Conclusions

Microstructural evolutionof the clad $Ti_{20}Zr_{20}Cu_{40}Ni_{20}$ metallic brazed CP-Ti alloy have been investigated composite joint brazed at 1270 K for 10 min. by using X-RD, DSC, FESEM and TEM. It is observed that the joint is dominated by primary β-Ti and coarse eutectic of (Ti, $Zr)_2Ni$, Ti_2Cu, and α-Ti during brazing. The primary β-Ti is transformed to fine lamellar eutectoid of (Ti, $Zr)_2Ni$, Ti_2Cu, Ti_2Ni, and α-Ti upon the subsequent cooling cycle of brazing. The loss of Cu, Ni and Zr from the braze melt results in isothermal solidification of molten braze, and the β-Ti grains dominate the entire joint at the brazing temperature. The β-Ti alloyed with Cu, Ni, and Zr is subsequently transformed to fine eutectoid of (Ti, $Zr)_2Ni$, Ti_2Cu, Ti_2Ni, and α-Ti.

Acknowledgements

AKB thanks the National Academy of Sciences, India (Allahabad) for the support through Senior Scientist Platinum Jubilee Fellowship. AKB also likes to thank for partial support from UGC-DAE-CSR (Mumbai) through project CRS-M199.

References

[1] R. Roger, E. W. Collings, and G. Welsch:Materials Properties Handbook: Titanium Alloys, asm International, Materials Park, Oh, 1993, Pp. 1–3.

[2] J. L. Walter, M. R. Jackson, and C. T. Sims: Titanium and Its Alloys: Principles of Alloying Titanium, asm International, Materials Park, Oh, 1988, pp. 23–33.

[3] J. R. Davis: asmHandbook, Volume 2: Properties and Selection: Nonferrous Alloys and Special Purpose Materials, asm International, Materials Park, Oh, 1990, Pp. 592–633.

[4] W. F. Smith: Structure and Properties of Engineering Alloys, Mcgraw-Hill Inc., New York, 1993, pp. 433–84.

[5] C. T. Chang, Y. C. Du, R. K. Shiue, and C. S. Chang:Mater. Sci. Eng., 2006, Vol. 420a, pp. 155–64.

[6] C. T. Chang, Z. Y. Wu, R. K. Shiue, and C. S. Chang: Mater. Lett, 2007, Vol. 61 (3), pp. 842–45.

[7] C. T. Chang, R. K. Shiue, and C. S. Chang: Scripta Mater., 2006, Vol. 54, pp. 853–58.

[8] Metallurgical and Materials Transactions A, (2013) 944a.

[9] Journal of Phase Equilibria and Diffusion, (2014) 2. 35.

[10] Materials Transactions (2008), Vol. 49, No. 6, pp. 1488.